DENTAL MATERIALS 35 (2019) 617–626

Available online at www.sciencedirect.com

ScienceDirect

journal homepage: www.intl.elsevierhealth.com/journals/dema

Monitoring demineralization and remineralization of human dentin by characterization of its structure with resonance-enhanced AFM-IR chemical mapping, nanoindentation, and SEM

Grigoriy Sereda[a,*], *Allison VanLaecken*[a], *Joseph Alan Turner*[b]

[a] *University of South Dakota, 414 E Clark St., Vermillion, SD 57069, United States*
[b] *University of Nebraska-Lincoln, 1400 R St., Lincoln, NE 68588, United States*

ARTICLE INFO

Article history:
Received 15 June 2018
Accepted 7 February 2019

Keywords:
Dentin
Tooth remineralization
Atomic force microscopy
Nanoindentation
Scanning electron microscopy
Collagen matrix

ABSTRACT

Objective. This research aimed at monitoring demineralization and remineralization of dentin and its collagen matrix at the nanoscale by amorphous, microcrystalline, and in situ formed hydroxyapatite.

Methods. The concurrent use of the resonance-enhanced atomic force microscopy coupled with infrared probe (AFM-IR) chemical mapping, nano-indentation, and scanning electron microscopy (SEM) provides a detailed insight into the structure of human dentin, as well as to the processes of its partial demineralization and remineralization.

Results. The resonance-enhanced AFM-IR chemical mapping of dentin has shown to be a useful method to follow distribution of its collagen and hydroxyapatite components at the micro- and nanoscale levels, especially in conjunction with SEM imaging and nanoindentation.

Dentin with a higher extent of natural dentin tubule occlusion tends to be harder and less elastic.

The relative affinity of the collagen and hydroxyapatite components of dentin toward hydroxyapatite depends on its type (amorphous, microcrystalline, or formed *in-situ*).

The gel mineralization technique allows for an even and controlled growth of hydroxyapatite guided by the completely demineralized collagen matrix of dentin.

Significance. The observed trends of the affinity of collagen toward different forms of hydroxyapatite helps develop new remineralizing formulations. The employed methods of characterization may provide an insight to the natural processes of bone mineralization guided by its both hydroxyapatite and protein constituents.

1. Introduction

The ongoing quest for new compositions able to remineralize human teeth requires new methods to monitor the intricate details of the remineralization process, especially, at the nanoscale level of the natural collagen bundles of dentin. The extent of remineralization is usually monitored by the com-

* *Corresponding author.*
E-mail address: gsereda@usd.edu (G. Sereda).
https://doi.org/10.1016/j.dental.2019.02.007

parison of the infrared absorption at 1525 cm^{-1} characteristic of the amide II C=O stretching band of collagen and at 1064 cm^{-1} characteristic of the phosphate-anion P=O stretching band of hydroxyapatite [1]. X-Ray diffraction (XRD) analysis and scanning electron microscopy (SEM) imaging have been also reported to characterize the morphology of the mineral component [2]. The distinctly different IR-absorptions of proteins (1585–1720 cm^{-1}) and phosphate (900–1200 cm^{-1}) allows for chemical mapping of organic and inorganic components of the bone under a microscope [3]. The recently developed instrumentation that couples atomic force microscopy (AFM) and InfraRred (IR) spectroscopy allows for the chemical mapping of components in biological materials, including dentin, at the nanoscale level [4]. The resonance-enhanced modification of the method features the IR-laser pulsed at a constantly re-tuned frequency of the oscillating AFM tip. This technique significantly increases both sensitivity (by a factor of 5–10) and lateral resolution (up to 10 nm or to the size of the AFM tip) [5]. This method, however, requires high quality polished specimens, which makes it unsuitable for analyzing soft collagen matrixes. The quality of mineralization that defines the mechanical properties of the mineral deposit calls for an alternative method as well. Here we report utilization of the resonance-enhanced AFM-IR spectroscopy in tandem with SEM imaging and nanoindentation to characterize different types of human dentin. This combination of methods was also used to monitor the mechanism of demineralization and remineralization of dentin and a dentin-derived collagen matrix at the nanoscale. The process of bone mineralization and remineralization that involves both mineral and organic components of the extracellular matrix [6], will be better understood with the suggested integrated approach to monitor its progress. It is already demonstrated that mineralization of bones with hydroxyapatite does not occur directly by the association of ions from solution, but rather proceeds through the step of formation of amorphous calcium phosphate. The exact mechanism of this transformation is currently under debate [6].

2. Materials and methods

2.1. Tooth specimen preparation

Tooth samples were collected, prepared, and cleaned by the method previously reported. [7] The enamel layer of the tooth specimens was removed to aid in sample processing except for one sample where the enamel was intentionally preserved for comparison. A tooth was mounted on a Beuhler Isomet Slow-speed saw, sectioned into 5 mm (0.3 mm thick) mid-coronal dentin slices with a diamond blade, rinsed with nanopure water, ultrasonicated for 1 h to remove saw smears and debris, and viewed with an *FEI Quanta 200 Environmental SEM* microscope to select the slices cut nearly perpendicular to the dentinal tubules, and determine the dentin type. The selected dentin slices were embedded to melted wax, cooled to the ambient temperature, and polished sequentially by 600 grit sandpaper, an aqueous slurry of 1 μm alumina particles, 0.3 μm, and finally, by 0.05 μm particles until the specimen looks shiny (usually 45 min). The wax was dissolved in acetone for 1 h, the dentin slice was ultrasonicated for 30 min, and dried at 100 °C for 5 min. For AFM-IR experiments, the specimen was mounted on a ZnS substrate with double-sided sticky carbon tape. For nanoindentation experiments, the specimen was glued to a steel disk with superglue.

2.2. Collagen matrix preparation

The collagen matrix was prepared by incubating a dentin slice in a phosphate buffer solution pH = 2 for 8 days (until pH stops to change in the process of hydroxyapatite leaching). The collagen matrix was a soft transparent material exhibiting a tubular structure under SEM. A lower voltage of 2 kV was necessary to minimize burning out of the material by the electron beam.

2.3. Instrumentation techniques

The AFM-IR experiments were performed on the *Anasys nanoIR2* instrument with an 80 nm Au-coated carbon tip and detection of IR absorption by the thermal expansion of the material under the tip in the contact mode. The nanoindentation experiments were performed on the *Hysitron TI 950 Triboindenter* with a Berkovitz tip applied at the maximum force of 4000 μN be a trapezoid load function 10 s, 5 s, 10 s. The value of the maximum force was experimentally selected from the area where the tip penetration depth does not significantly depend on the applied force.

2.4. Gel diffusion method

The gel diffusion remineralization was performed by the diffusion of calcium and phosphate ions through a phosphate-linked chitosan gel by the following procedure: A solution of 1 g of chitosan in 49 mL of 0.5% aqueous acetic acid was prepared by stirring for 4 h or until the bubbles were mostly removed from the degassed solution. While stirring, the degassed chitosan/acetic acid solution was brought to Õ °C. Next, 5 mL of an aqueous Na_2HPO_4 (500 mg/mL) solution was added dropwise to the chitosan solution. The solution turned to a viscous opalescent, but free-flowing liquid (gel precursor), which was stored at Õ °C. A dentin specimen was placed in a glass elbow filled with the gel precursor. The gel was formed by warming the glass elbow to 37 °C in a water bath for 10–15 min. The glass elbow joints were connected with two flasks filled with 0.5M Na_2HPO_4 and 0.5M $CaCl_2$ correspondingly. The assembly was flipped to place the flasks at the top and allow gravity diffusion of ions through the gel. After 24 h, the dentin slice was removed from the gel, rinsed with nanopure water until the gel is removed, and dried on air.

3. Results

3.1. Characterization of different types of dentin

First, we have harnessed capabilities of the proposed integrated method of characterization by analyzing chemical and morphological features of four types of dentin: (a) Dentin from caries-free teeth with unoccluded dentinal tubules, (b)

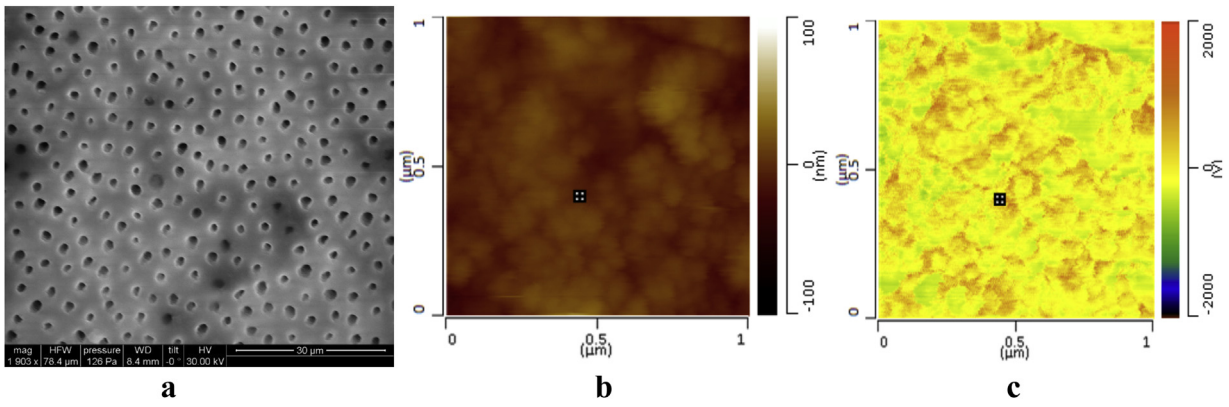

Fig. 1 – (a) SEM image of dentin from caries-free teeth with unoccluded dentinal tubules. (b) AFM topography map of caries-free dentin with unoccluded dentinal tubules. (c) Hydroxyapatite chemical map at 1024 cm^{-1} of caries-free dentin with unoccluded dentinal tubules (For interpretation of the references to colour in the text, the reader is referred to the web version of this article).

Dentin from caries-free teeth with the dentinal tubules partially occluded, (c) Dentin from caries teeth with the dentinal tubules partially occluded, and (d) Dentin visibly damaged with 5–15 μm black spots.

3.1.1. *Dentin from caries-free teeth with unoccluded dentinal tubules (Fig. 1)*

The AFM topography map of a 1 × 1 μm area (Fig. 1b) reveals collagen bundles characteristic for the nanoscale structure of dentin. [8] The square mark placed on the same location in images b and c allowed us to relate the chemical and the topography maps. The chemical map of hydroxyapatite recorded at 1024 cm^{-1} characteristic for the phosphate-anion (Fig. 1c) shows higher adsorption by the red areas and lower adsorption by the yellow areas, according to the color legend on the right side of the image. The red area on the right side from the mark placed at the edge of a collagen bundle indicates higher abundance of hydroxyapatite between the collagen bundles than over the bundles. The same trend was observed throughout the sample. The wavenumber for the chemical map of hydroxyapatite has been matched with the maximum of the phosphate-ion absorption [1] in the area 1000–1070 cm^{-1}.

Table 1 – Mechanical properties of dentin with different extents of dentinal tubule occlusion.

	Young's modulus (GPa)	Hardness (GPa)
No occlusion	21 +/−2	0.9 +/−0.2
Partial occlusion (caries-free dentin)	27 +/−2	1.1 +/−0.1
Partial occlusion (caries dentin)	30 +/−4	1.4 +/−0.3
Complete occlusion (damaged dentin)	33 +/−4	1.6 +/−0.4

The nanoindentation experiments did not reveal any significant dependence of the Young's modulus and hardness of dentin on the distance from the tubules. Over 18 measurements, the average Young's modulus summarized in Table 1, was found to be consistent with literature data. [9]

3.1.2. *Dentin from caries-free teeth with the dentinal tubules partially occluded (Fig. 2)*

The chemical map 1024 cm^{-1} of a 1.5 × 1.5 μm area shows that similarly to the dentin with not occluded tubules, hydroxyapatite tends to be mostly distributed between the collagen

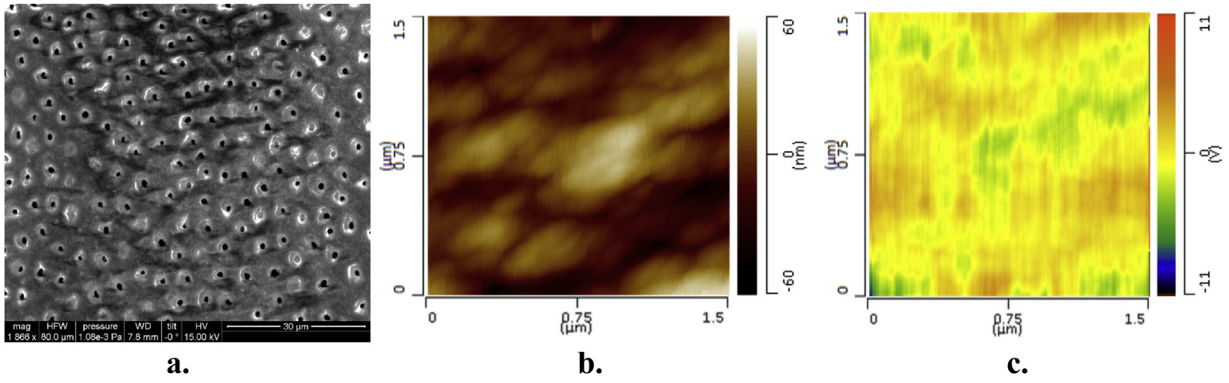

Fig. 2 – (a) SEM image of dentin from caries-free teeth with the dentinal tubules partially occluded. (b) AFM topography map of caries-free dentin with the dentinal tubules partially occluded (dentin area). (c) Hydroxyapatite chemical map at 1024 cm^{-1} of caries-free dentin with the dentinal tubules partially occluded (dentin area) (For interpretation of the references to colour in the text, the reader is referred to the web version of this article).

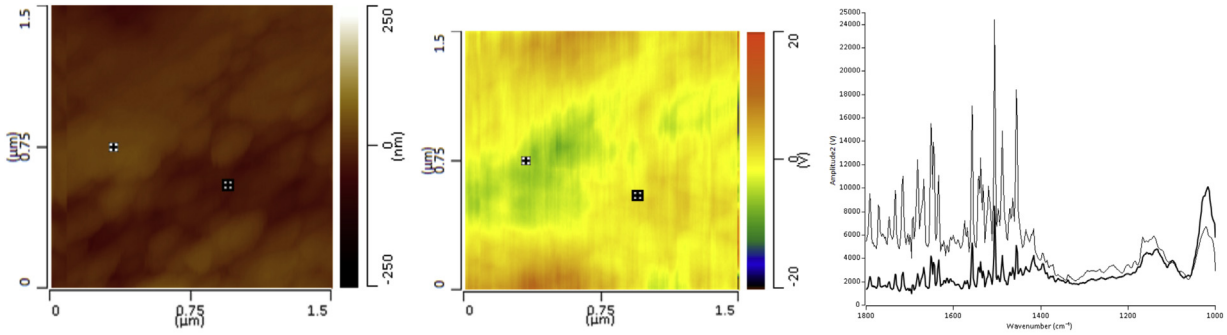

Fig. 3 – (a) AFM topography map of caries-free dentin with the dentinal tubules partially occluded (enamel area). (b) Hydroxyapatite chemical map at 1024 cm^{-1} of caries-free dentin with the dentinal tubules partially occluded (enamel area). (c) IR-spectra taken at the locations shown in Fig. 3 (a,b) The highlighted spectrum corresponds to the darker location mark (For interpretation of the references to colour in the text, the reader is referred to the web version of this article).

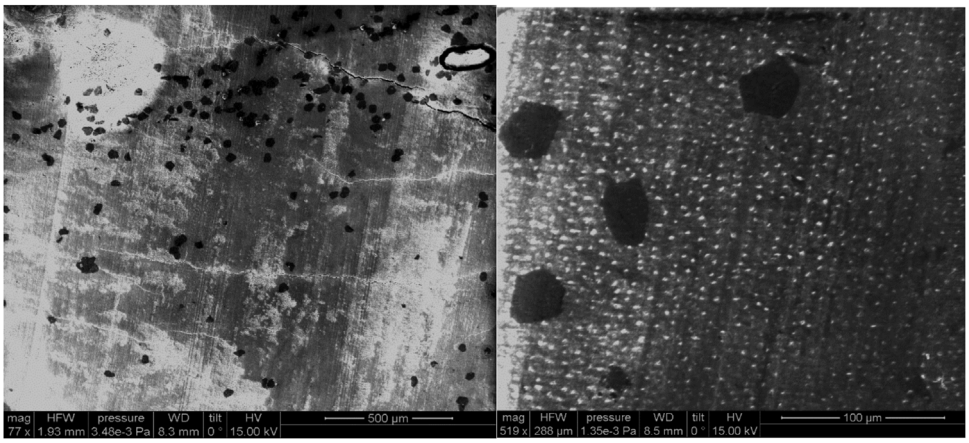

Fig. 4 – SEM images of dentin with the damaged areas visible as black spots.

bundles: the darker areas on the topography map correlate with the red areas on the chemical map (Fig. 2b,c). In the enamel area of the specimen, hydroxyapatite was also more abundant in higher topography areas (Fig. 3a,b). The validity of the chemical map has been verified by two overlaid IR-spectra (Fig. 3c) taken in the locations marked on Fig. 3a,b. The highlighted spectrum corresponds to the location with higher abundance of hydroxyapatite marked by the right square in the darker area of the topography map and the light-red area of the chemical map.

The average Young's modulus and hardness measured in 5 points and summarized in Table 1, show that partial occlusion of dentinal tubules seems to make dentin harder and less elastic. However, further research is necessary to address the individual variations of mechanical properties of the specimens.

3.1.3. *Dentin from caries teeth with the dentinal tubules partially occluded*

The SEM, AFM-IR images and nanoindentation data (Table 1) of this type of dentin looked very similar to their occluded counterparts from caries-free teeth.

3.1.4. *Dentin visibly damaged with 10–500 μm black spots (Fig. 4)*

The damaged dentin is characterized by the presence of black areas and complete occlusion of dentinal tubules. The eight nanoindentation measurements further confirmed that higher extents of dentinal tubule occlusion are characteristic for less elastic and harder dentin (Table 1).

The Table 1 summarizes mechanical properties of several types of dentin.

The black areas of the damaged dentin crumbled and were so soft, that even at the load of 100 μN, the tip consistently penetrated the surface by more than 2 μm, and we could not obtain any reliable numerical data for those areas.

The distribution of hydroxyapatite in the highly occluded dentin area outside of the black spots was different than in the unoccluded or slightly occluded samples. The chemical map at 1024 cm^{-1} revealed depositions of hydroxyapatite at the ridge (marked by a black curve) of an almost completely occluded tubule (Fig. 5a,b). The hydroxyapatite deposition area inside the occluded tubule is marked by a diamond.

The hydroxyapatite chemical map of a 1×1 μm area of highly occluded dentin shows that hydroxyapatite tends to be

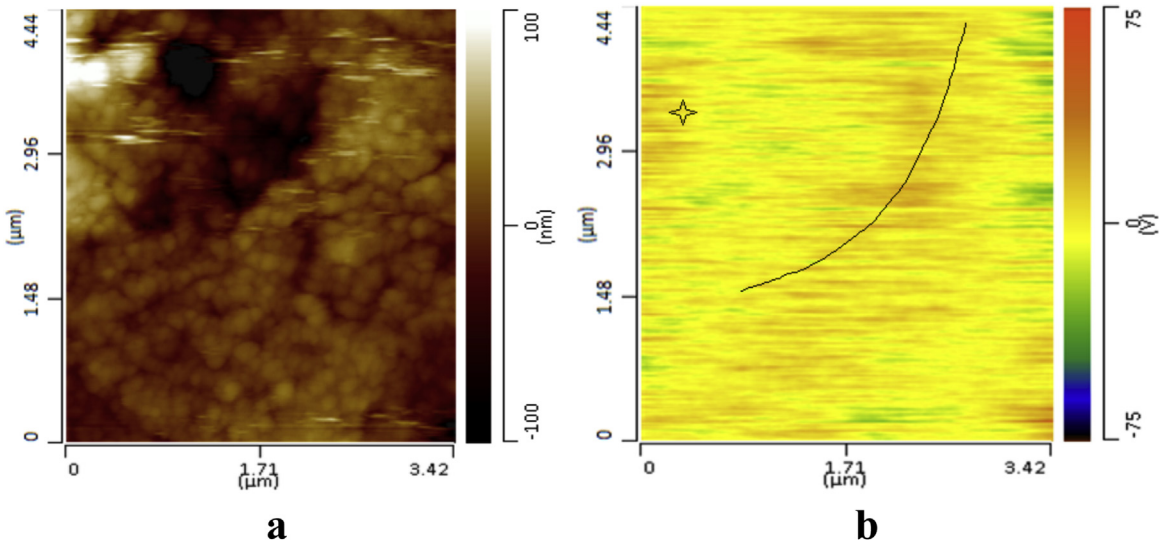

Fig. 5 – (a) AFM topography map of damaged dentin (outside of black spots area). (b) Hydroxyapatite chemical map at 1024 cm^{-1} of damaged dentin (outside of black spots area).

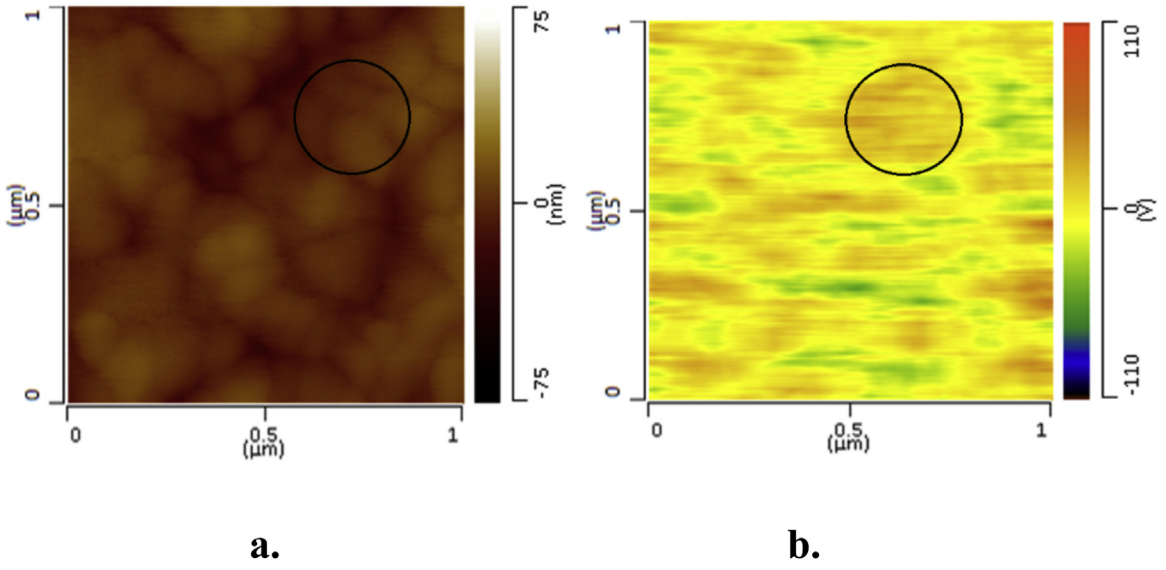

Fig. 6 – (a) 1 × 1 µm AFM topography map of damaged dentin (outside of black spots area). (b) 1 × 1 µm Hydroxyapatite chemical map at 1024 cm^{-1} of damaged dentin (outside of black spots area).

present on the bundles of collagen (Figs. 6a,b), contrary to the not occluded dentin with hydroxyapatite deposits between the collagen bundles. In Fig. 6, one of the areas of hydroxyapatite deposition is circled on the chemical map, as well as the area of collagen bundles on the topography map.

The IR spectra taken inside a black spot have revealed that hydroxyapatite has been almost completely leached from those areas (Fig. 7a).

The high intensity of a group of signals characteristic for amides has allowed us to map the abundance of amides inside the black spot area of the damaged dentin (Fig. 7b,c).

The mapped distribution of amides (Fig. 7b,c) is consistent with the local IR-spectra (Fig. 7a). The highlighted spectrum in Fig. 7a corresponds to the darker location in Fig. 7b,c.

3.2. *Demineralization of dentin*

Next, we applied the combination of AFM-IR, SEM, and nanoindentation to monitor demineralization of dentin. The procedure for partial demineralization was similar to that reported in the literature [1], and consisted in the incubation of a dentin slice in a phosphate buffer solution at pH = 4.5 for 3 days.

The SEM image has shown visible deterioration of dentin, especially, at the edges of dentinal tubules (Fig. 8a).

A series of local IR spectra revealed the most intensive absorption in the hydroxyapatite area at 1128 cm^{-1}, which might be due to various phosphate-anions adsorbed from the buffer solution. Incubation of the sample in deionized

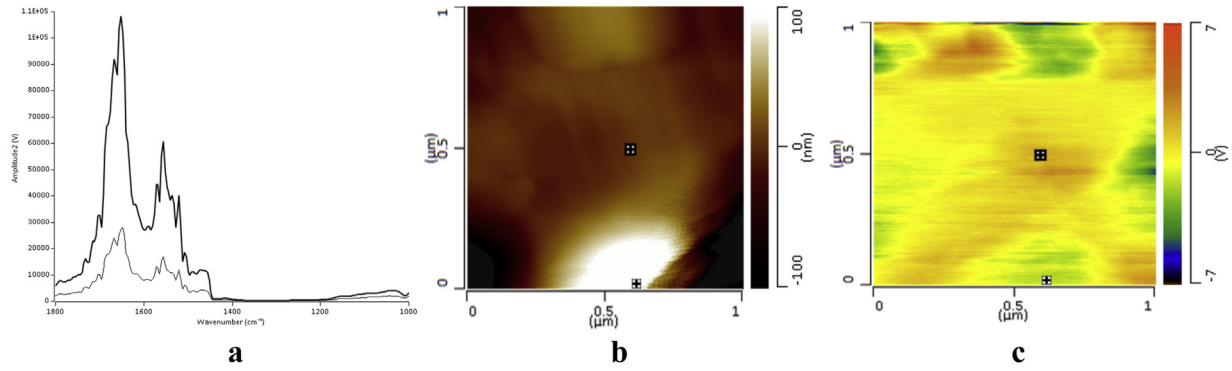

Fig. 7 – (a) IR spectra taken at two locations inside the black spot area marked in Fig. 7b,c. (b) AFM topography map of damaged dentin (inside the black spots area). (c) The amide chemical map at 1652 cm^{-1} of damaged dentin (inside the black spots area).

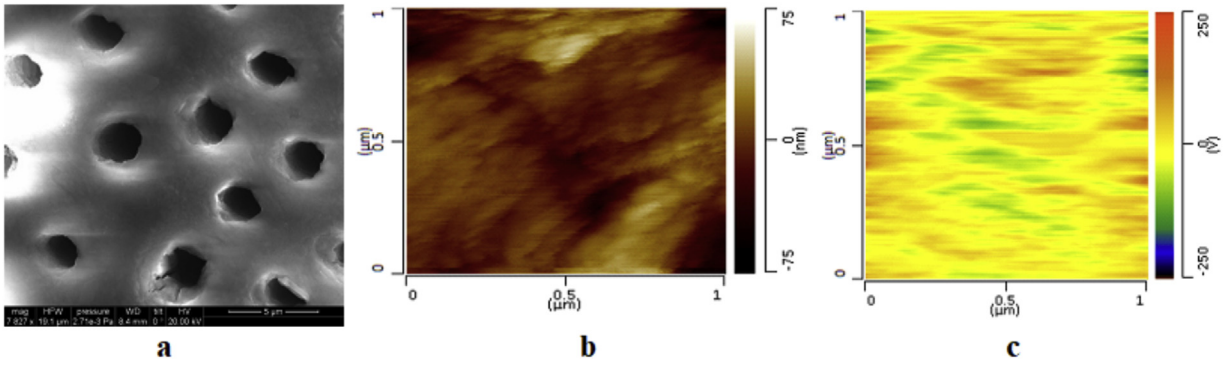

Fig. 8 – (a) SEM micrograph of partially demineralized dentin. (b) AFM topography map of partially demineralized dentin. (c) The hydroxyapatite chemical map at 1024 cm^{-1} of partially demineralized dentin.

water for 2 days significantly decreased this band and allowed us confidently monitor the hydroxyapatite absorption at 1024 cm^{-1}. Over 8 measurements, the average Young's modulus was found to be 3 +/−1 GPa, and the average hardness was found to be 0.09 +/−0.04 GPa.

3.3. *Remineralization of dentin*

3.3.1. *Remineralization of dentin by the MI toothpaste*

MI toothpaste is the first toothpaste approved for tooth remineralization. It is action based on a complex of amorphous hydroxyapatite with phosphoproteins isolated from milk, which supplies the essential precursor of remineralization to the tooth surface. [10] The deposition of hydroxyapatite on partially remineralized dentin by the MI toothpaste during a 5 min exposure has been proved by the ATR-IR spectroscopy of the bulk surface [1]. We repeated that procedure of remineralization by the MI toothpaste (application of the toothpaste to the dentin slice for 5 min, followed by rinsing with water), and characterized the process by SEM, AFM-IR, and nanoindentation. The SEM image has shown visible deposition on the surface and partial occlusion of some tubules (Fig. 9a).

Over 8 measurements, the average Young's modulus was found 3 +/−1 GPa, and the average hardness was found 0.17 +/−0.09 GPa.

The hydroxyapatite chemical map at 1024 cm−1 provides unique information that deposition of hydroxyapatite by the MI toothpaste occurs both between, and on the collagen bundles (Fig. 9 a,b).

3.3.2. *Remineralization of dentin by the Colgate® toothpaste with 5% of hydroxyapatite*

Another type of remineralizing toothpastes (for example, Biorepair®) utilizes nanoparticles of hydroxyapatite as an active ingredient, delivering the remineralizing precursor to the tooth surface [11]. This composition was modeled by grinding a commercially available Colgate® toothpaste with 5% wt of hydroxyapatite supplement.

The SEM image has shown that hydroxyapatite mostly deposits in the dentinal tubules (Fig. 10).

Over 8 measurements, the average Young's modulus was found 3 +/−1 GPa, and the average hardness was found 0.12 +/−0.08 GPa.

The hydroxyapatite chemical map at 1024 cm^{-1} revealed a very similar distribution of the deposited hydroxyapatite to that induced by the MI® toothpaste.

3.3.3. *Remineralization of dentin by the gel diffusion method*

The SEM image shows significant depositions throughout the sample. Most tubules are occluded (Fig. 11a).

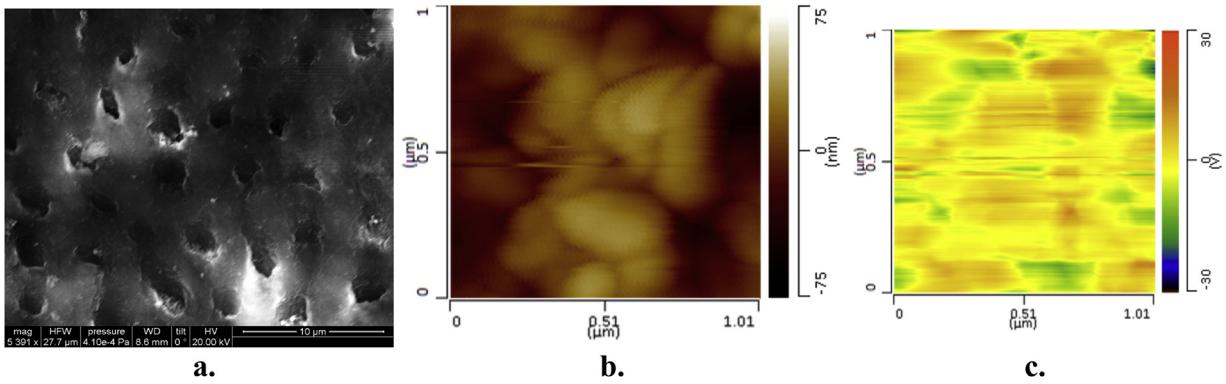

Fig. 9 – (a) SEM micrograph of partially demineralized dentin remineralized by the MI toothpaste. (b) AFM topography map of partially demineralized dentin remineralized by the MI toothpaste. (c) The hydroxyapatite chemical map at 1024 cm^{-1} of partially demineralized dentin remineralized by the MI toothpaste.

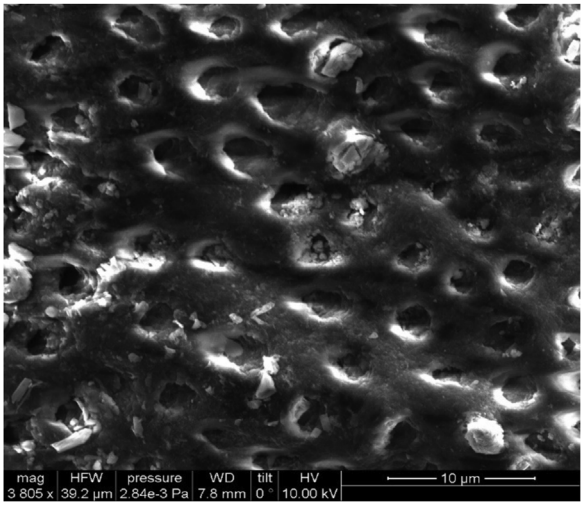

Fig. 10 – SEM micrograph of partially demineralized dentin remineralized by a toothpaste with 5% of hydroxyapatite.

The hydroxyapatite chemical map at 1024 cm^{-1} shows most of the deposited hydroxyapatite on the higher topography areas, which is consistent with the preferred deposition of hydroxyapatite on the collagen bundles than on the existing hydroxyapatite areas between them (Figs. 11b,c).

Over 8 measurements, the average Young's modulus was found 6 +/−3 GPa, and the average hardness was found 0.2 +/−0.1 GPa. The mechanical properties of the initial, demineralized, and remineralized dentin are summarized in Table 2.

3.4. *Remineralization of collagen matrix by the gel diffusion method*

The collagen matrix (Fig. 12) was prepared by demineralization of a dentin slice in an aqueous acidic solution (pH = 2) until the pH of the solution stabilizes due to the complete dissolution of the hydroxyapatite component of dentin.

Remineralization of the collagen matrix in a chitosan-phosphate gel by the counter-diffusion of calcium and phosphate ions for 24 h lead to patchy deposits of hydroxyapatite mostly in collagen wrinkles. The deposits did not show a noticeable particulate structure (Fig. 13).

The further mineralization for another 24 h under the same conditions lead to the formation of hydroxyapatite microcrystals (Fig. 14). Significant deposition was observed inside the dentinal tubules, which lead to their partial or full occlusion.

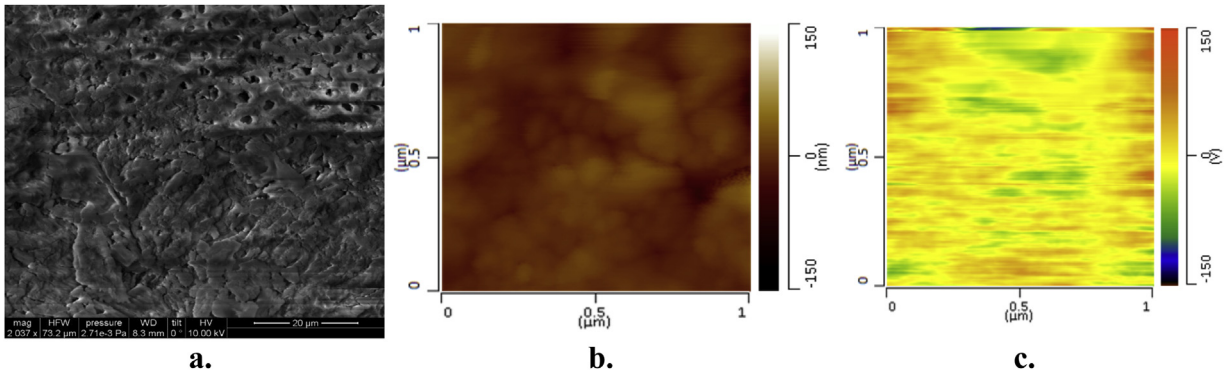

Fig. 11 – (a) SEM micrograph of partially demineralized dentin remineralized by the gel diffusion method. (b) AFM topography map of partially demineralized dentin remineralized by the gel diffusion method. (c) The hydroxyapatite chemical map at 1024 cm^{-1} of partially demineralized dentin remineralized by the gel diffusion method.

Table 2 – Mechanical properties of the initial, demineralized, and remineralized dentin.

	Young's modulus (GPa)	Hardness (GPa)
Initial dentin	21 +/−2	0.9 +/−0.2
Partially demineralized dentin	3 +/−1	0.09 +/−0.04
Dentin remineralized by the MI paste	3 +/−1	0.17 +/−0.09
Dentin remineralized with Colgate-hydroxyapatite toothpaste	3 +/−1	0.12 +/−0.08
Dentin remineralized by gel diffusion	7 +/−3	0.2 +/−0.1

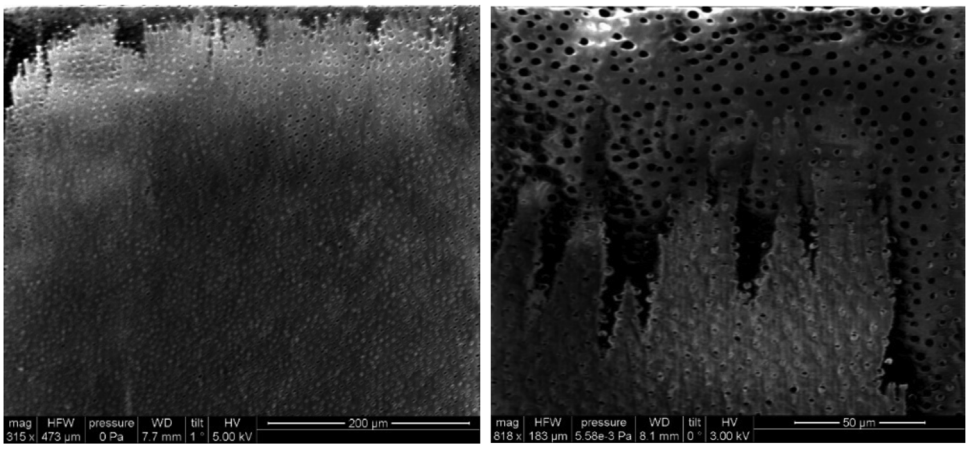

Fig. 12 – SEM images of the collagen matrix.

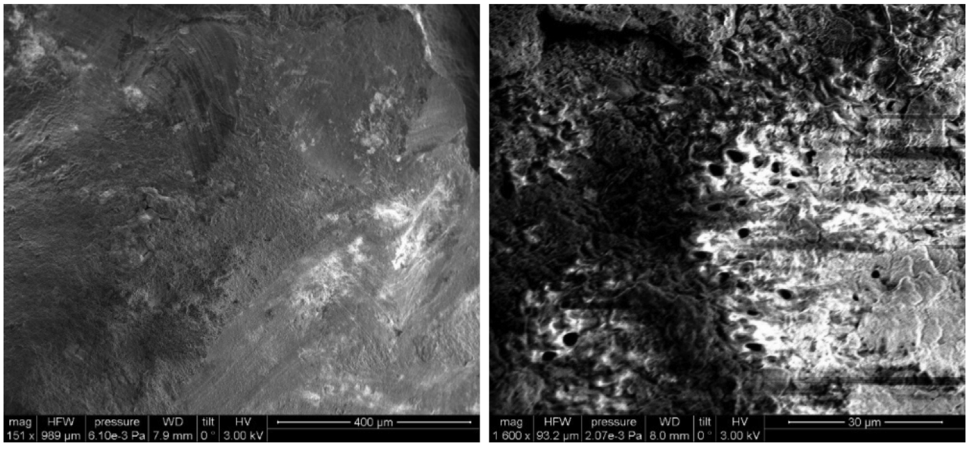

Fig. 13 – SEM images of the collagen matrix mineralized for 24 h.

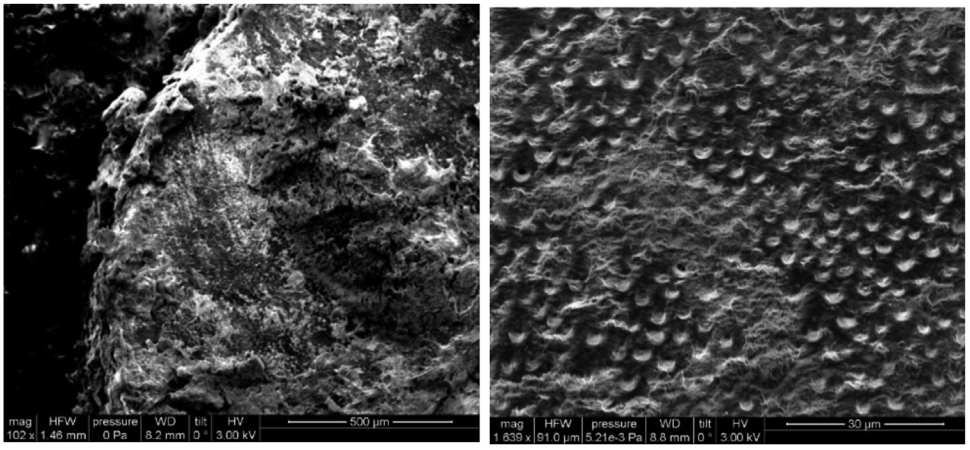

Fig. 14 – SEM images of the collagen matrix mineralized for 48 h.

4. Discussion

4.1. Characterization of dentin

For both healthy and caries-affected dentin, regardless of the extent of dentinal tubule occlusion, we observed higher abundance of hydroxyapatite between the collagen bundles than over the bundles. Interestingly, an enamel area of a tooth slice revealed a very similar pattern of hydroxyapatite and collagen to that in dentin, despite the known fact [12] of higher mineralization of enamel vs. dentin. In the damaged dentin, the deposition pattern of hydroxyapatite on the surface was reversed: most of the mineral was deposited over the collagen bundles. Together with the highest extent of dentinal tubule occlusion, this points to the natural over-mineralization of the damaged dentin. This is consistent with a literature report that natural occlusion of dentinal tubules is a part of the protective mechanism from the tooth damage [13]. Further, the natural over-mineralization affect the mechanical properties of dentin, making it harder and less elastic. The Young's modulus gradually increased from 21 GPa to 33 GPa, and the hardness increased from 0.9 GPa to 1.6 GPa in the series: normal not occluded dentin, normal occluded dentin, caries-affected dentin (always occluded), and damaged dentin (always occluded) (Table 1). In all cases, the mechanical microscale mechanical properties of dentin did not significantly depend on the distance from a dentinal tubule. However, both chemical composition and mechanical properties of the black areas of the damaged dentin were distinctly different from the rest of the dentin surface. The IR spectra taken inside a black spot revealed that hydroxyapatite has been almost completely leached from those areas (Fig. 7a). The observed depletion of hydroxyapatite is consistent with a remarkable softness of the material, according to the nanoindentation experiments. In those areas, we observed much higher abundance of amides, which are likely to belong to either collagen or its products of decay.

4.2. Demineralization of dentin

When the FTIR method is used to monitor demineralization of dentin in a phosphate buffer, a care should be taken to avoid artifacts from the phosphate-ions absorbed by dentin from the solution. It is important to incubate the specimen in deionized water for 2 days to remove the adsorbed phosphate. After partial demineralization, hydroxyapatite still had a slight tendency to be more persistent in the areas between collagen bundles, but this trend is now almost nonexistent due to the preferential dissolution of hydroxyapatite between the collagen bundles (Figs. 8b,c). Therefore, hydroxyapatite bound with collagen dissolves slower, which implies that the collagen-hydroxyapatite complex resists demineralization. As expected, the partial loss of hydroxyapatite during demineralization significantly increased elasticity and decreased hardness of dentin. The Young's modulus fell from 21 GPa to 3 GPa, and the hardness fell from 0.9 GPa to 0.09 GPa (Table 2).

4.3. Remineralization of dentin

Remineralization with the MI toothpaste deposited hydroxyapatite on the surface and inside of some tubules (Fig. 9a), while treatment by the Colgate-hydroxyapatite toothpaste mostly deposits microcrystals of hydroxyapatite (geometrically matching the tubule opening size) in the tubules (Fig. 10). The higher affinity of the amorphous hydroxyapatite component of the MI toothpaste to dentin compared with microcrystalline hydroxyapatite is consistent with its higher chemical potential characteristic for amorphous materials. According to the FTIR chemical maps (Figs. 9), for either MI or the Colgate-hydroxyapatite toothpaste, deposition of hydroxyapatite occurs both between and on the collagen bundles. The nanoindentation experiments have revealed that, in either case, the deposited hydroxyapatite did not change the Young's modulus of the dentin surface and resulted in just a marginal increase of hardness (Table 2). Therefore, the deposited hydroxyapatite did not integrate into the structure of dentin, but rather supplied the precursors for further remineralization to the tooth surface.

As opposed to the introduction of either amorphous or crystalline hydroxyapatite to the dentin surface, the gel diffusion method supplies ions of calcium and phosphate there, which form hydroxyapatite on the surface. The SEM image shows significant depositions throughout the sample and occlusion of most dentinal tubules (Fig. 11a). Interestingly, the gel diffusion method preferentially deposits hydroxyapatite on the collagen bundles rather than on the existing hydroxyapatite areas between them (Figs. 11b,c). This may be due to the affinity of calcium ions to the dentin phosphoproteins [13], which leads to their preferential binding with the organic matrix of dentin, followed by the growth of hydroxyapatite. The nanoindentation experiments have revealed that contrary to the application of the MI and hydroxyapatite toothpaste, deposition of hydroxyapatite by the gel diffusion method noticeably increases both Young's modulus and hardness of demineralized dentin but does not bring them even close to the values of the initial dentin (Table 2).

Comparison of the three methods of hydroxyapatite deposition speaks to the best effectiveness of the gel diffusion method, which advances the process most toward remineralization.

4.4. Remineralization of the collagen matrix

With the purpose of looking at the role of the collagen component alone in the process of remineralization, the same gel diffusion mineralization procedure was applied to the collagen matrix. The prepared collagen matrix retains the major morphology feature of the original dentin — its dentinal tubules. However, it was not flat enough to be analyzed by AFM or nanoindentation. Therefore, remineralization of the collagen matrix was monitored solely by SEM. Gel remineralization of the collagen matrix for 24 h lead to patchy deposits of hydroxyapatite observed mostly in collagen wrinkles. The deposits did not show a noticeable particulate structure (Fig. 13). The noticeable deposition and relatively even distribution of hydroxyapatite on the collagen matrix is consistent with the increased affinity of the *in-situ* formed hydroxya-

patite to the collagen component of dentin (Fig. 11). The continued remineralization led to the formation of hydroxyapatite microcrystals, seeded by the initially formed mineral layer (Fig. 14). Significant deposition of hydroxyapatite was observed inside the dentinal tubules, which led to their partial or full occlusion.

These observations signify the role of the binding of calcium ions to the dentin organic matrix in the tooth remineralization process.

5. Conclusions

The resonance-enhanced AFM-IR chemical mapping of dentin has shown to be a useful method to follow the distribution of its collagen and hydroxyapatite components at the micro- and nanoscale levels, especially in conjunction with SEM imaging and nanoindentation. While SEM is convenient to monitor mineralization of a soft and uneven collagen matrix, nanoindentation is a sensitive method for detecting partial demineralization of dentin by acidic leaching of hydroxyapatite.

Regardless of the type of dentin, its Young's modulus and hardness noticeably vary for different locations on the surface, but do not significantly depend on the distance from a dentinal tubule. Dentin with a higher extent of natural dentin tubule occlusion tends to be harder and less elastic.

Hydroxyapatite is almost completely depleted in the visible black areas of damaged dentin, which is consistent with the extreme mechanical weakness of those areas.

Application of a formulation with amorphous or microcrystalline hydroxyapatite to dentin results in the deposition of hydroxyapatite on both collagen bundles and the hydroxyapatite crystals between them. In contrast, hydroxyapatite formed by diffusion of calcium and phosphate ions through a gel, preferably deposits on the collagen bundles, giving rise to the subsequent growth of the more mechanically robust mineral deposit. The gel mineralization technique allows for an even and controlled growth of hydroxyapatite guided by the completely demineralized collagen matrix of dentin.

6. Data availability

The raw and processed data required to reproduce these findings are available to download from https://data.mendeley.com/datasets/v8hjj9r93c/1.

Acknowledgements

The research was performed in part at the Nebraska Nanoscale and NanoEngineering Research Core Facilities: National Nanotechnology Coordinated Infrastructure and the Nebraska Center for Materials and Nanoscience, which are supported by the National Science Foundation under Award ECCS: 1542182, and the Nebraska Research Initiative. We thank Dr. Joshua Brower (SmilesForSiouxland) for financial support and for the help in the acquisition and preparation of tooth specimens. We also thank Brandon Karels for the development of the procedure of the gel remineralization.

REFERENCES

[1] Rahiotis Ch, Vougiouklakis G. Effect of a CPP-ACP agent on the demineralization and remineralization of dentine in vitro. J Dent 2007;35:695–8.
[2] Ruan Q, Liberman D, Bapat R, Chandrababu KB, Phark JH, Moradian-Oldak J. Efficacy of amelogenin-chitosan hydrogel in biomimetic repair of human enamel in pH-cycling systems. J Biomed Eng Inf 2016;2(1):119–28.
[3] Boskey AL. Mineralization of bones and teeth. Elements 2007;3:387–93.
[4] Amarie S, Zaslansky P, Kajihara Y, Griesshaber E, Schmahl WW, Keilmann F. Nano-FTIR chemical mapping of minerals in biological materials. Beilstein J Nanotechnol 2012;3:312–23.
[5] Anasys Intuments. Resonance-enhanced AFM-IR: https://www.anasysinstruments.com/resonance-enhanced-afm-ir-2/. [Last Accessed 15 August 2017].
[6] Neel E, Aljabo A, Strange A, Ibrahim S, Coathup M, Young A, et al. Demineralization–remineralization dynamics in teeth and bone. Int J Nanomed 2016;11:4743–63.
[7] Rashwan K, Sereda G. Applications of nanoparticles through surface functionalization. Nanotechnology: Delivering on the Promise, vol. 2. American Chemical Society; 2016. p. 91–105.
[8] Habelitz S, Balooch M, Marshall SJ, Balooch G, Marshall GW. In situ atomic force microscopy of partially demineralized human dentin collagen fibrils. J Struct Biol 2002;138:227–36.
[9] Kinney JH, Balooch M, Marshall SJ, Marshall GW, Weihs TP. Hardness and Young's modulus of human peritubular and intertubular dentine. Arch Oral Biol 1996;41(1):9–13.
[10] Gurunathan D, Somasundaram S, Kumar SA. Casein phosphopeptide-amorphous calcium phosphate: a remineralizing agent of enamel. Aust Dent J 2012;57:404–8.
[11] Tschoppe P, Zandim DL, Martus P, Kielbassa AM. Enamel and dentine remineralization by nano-hydroxyapatite toothpastes. J Dent 2011;39:430–7.
[12] Goldberg M, Kulkarni AB, Young M, Boskey A. Dentin: structure, composition and mineralization. Front Biosci (Elite Ed) 2011;3:711–35.
[13] Nakajima M, Kunawarote S, Prasansuttiporn T, Tagami J. Bonding to caries-affected dentin. Jpn Dent Sci Rev 2011;47:102–14.